Title

Fluorescent Biosensors for Multiplexed Imaging of Phosphoinositide Dynamics.

Journal

ACS Chemical Biology, 15(1)

Authors

Hertel, Fabian
Li, Simin
Chen, Mingyuan
et al.

Publication Date

2020-01-17

DOI

10.1021/acschembio.9b00691

Peer reviewed

HHS Public Access

Author manuscript

ACS Chem Biol. Author manuscript; available in PMC 2020 April 21.

Published in final edited form as:

ACS Chem Biol. 2020 January 17; 15(1): 33–38. doi:10.1021/acschembio.9b00691.

Fluorescent Biosensors for Multiplexed Imaging of Phosphoinositide Dynamics

Fabian Hertel[†,∇,⊥], **Simin Li**[†,⊥], **Mingyuan Chen**[‡], **Lutz Pott**[‖], **Sohum Mehta**[†], **Jin Zhang**[*,†,‡,§]

[†]Department of Pharmacology, University of California San Diego, La Jolla, California 92093, United States

[‡]Department of Bioengineering, University of California San Diego, La Jolla, California 92093, United States

[§]Department of Chemistry and Biochemistry, University of California San Diego, La Jolla, California 92093, United States

[‖]Institute of Physiology, Ruhr-University Bochum, 44801 Bochum, Germany

Abstract

Phosphoinositides constitute a critical family of lipids that regulate numerous cellular processes. Phosphatidylinositol 4,5-bisphosphate (PIP_2) is arguably the most important plasma membrane phosphoinositide and is involved in regulating diverse processes. It is also the precursor of phosphatidylinositol 3,4,5-trisphosphate (PIP_3), which is critical for growth factor signaling, as well as membrane polarization and dynamics. Studying these lipids remains challenging, because of their compartmentalized activities and location-dependent signaling profiles. Here, we introduce several new genetically encoded fluorescent biosensors that enable real-time monitoring of PIP_2 levels in live cells, including FRET-based and dimerization-dependent fluorescent protein (ddFP)-based biosensors that enable real-time monitoring of PIP_2 levels in live cells. In addition, we developed a red fluorescent biosensor for 3-phosphoinositides that can be co-imaged with the green PIP_2 indicator. Simultaneous visualization of dynamics of PIP_2 and 3-phosphoinositides in the same cell shows that plasma membrane PIP_3 formation upon EGF stimulation is coupled to a decrease in the local pool of PIP_2.

Graphical Abstract

[*]**Corresponding Author:** jzhang32@ucsd.edu.

[∇]**Present Address:** Department of Nuclear Medicine, University Hospital RWTH Aachen, Aachen, Germany.

[⊥]These authors contributed equally to this work.

Author Contributions

F.H., S.L., L.P., and J.Z. designed the experiments. F.H., S.L., and M.C. performed research. F.H., S.L., M.C., S.M., and J.Z. analyzed data. F.H., S.L., S.M., and J.Z. wrote the paper.

Supporting Information

The Supporting Information is available free of charge at https://pubs.acs.org/doi/10.1021/acschembio.9b00691.

Figures S1–S14 (PDF)

The authors declare no competing financial interest.

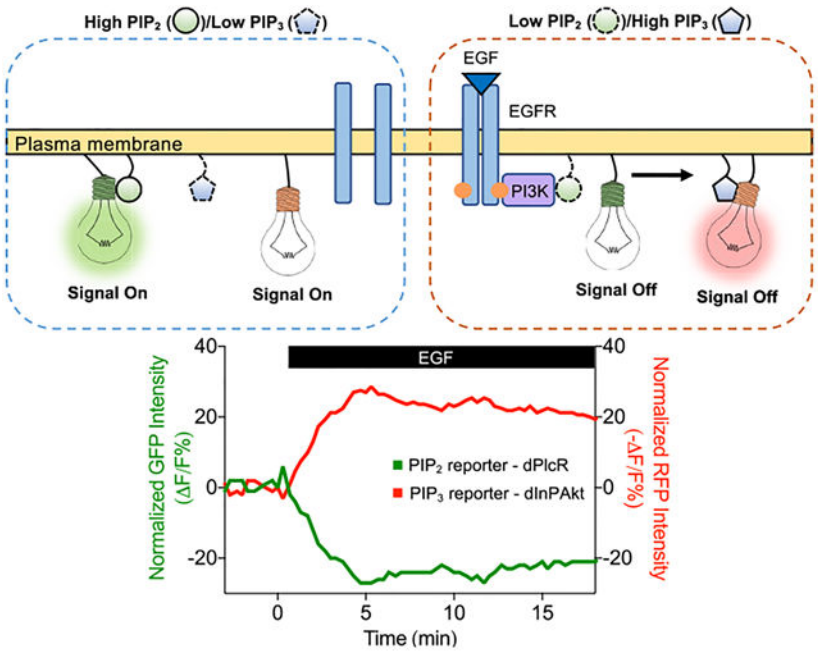

INTRODUCTION

Phosphoinositides belong to the class of glycerophospholipids, consisting of a glycerol backbone connected to two fatty acids and an inositol headgroup through a phosphate group. Although they comprise only a small fraction of the phospholipids in cellular membranes, these lipids play a critical role for several cellular processes.[1] The most important phosphoinositide species in the inner leaflet of the plasma membrane are phosphatidylinositol 4,5-bisphosphate (PIP_2) and phosphatidylinositol 3,4,5-trisphosphate (PIP_3), which are regulated differently and correspondingly fulfill different roles. The more abundant PIP_2 serves as a plasma-membrane-anchoring molecule for numerous proteins to facilitate their biological functions and also can be hydrolyzed by phospholipase C (PLC) to produce inositol trisphosphate (IP_3) and diacylglycerol (DAG) as part of the G_q signaling pathway.[2] In contrast, the plasma membrane concentration of 3-phosphorylated phosphoinositide species, including PIP_3 and $PI(3,4)P_2$, is low in resting cells and tightly controlled by lipid phosphatases such as Phosphatase and Tensin Homologue (PTEN). Upon stimulation of growth factor receptors and activation of Phosphoinositide 3-Kinase (PI3K), $PI(3,4)P_2$ and PIP_3 are rapidly produced in the plasma membrane, exhibiting the typical characteristics of second messengers. Several signaling pathways rely on the recruitment of enzymes and adaptor proteins to the membrane through specific interactions with these phosphoinositides. Overall, signaling involving these phosphoinositides is linked to several cellular processes, including metabolism, survival, proliferation, apoptosis, growth, and cell migration.[3]

Utilizing phosphoinositide-specific binding domains, several genetically encodable biosensors have been developed for monitoring these lipids.[4] The first class of biosensors has been generated through the straightforward fusion of a fluorescent protein (FP) to

binding domains such as pleckstrin homology (PH) domains so that changes in membrane concentrations of the target phosphoinositides result in FP translocation from or to the membrane, which can be observed and quantified through the change in fluorescence intensity at the membrane.[5] Utilizing the same PH domains to recognize phosphoinositides, Förster resonance energy transfer (FRET)-based reporters have been developed where YFP- and CFP-tagged PH domains undergo FRET, the efficiency of which is determined by their density at the plasma membrane and, thus, reflects plasma membrane phosphoinositide levels.[6] However, these translocation-based reporters rely on free diffusion to indicate phosphoinositide level changes and cannot be targeted to a desired subcellular location to monitor compartmentalized signaling. Later, FRET-based unimolecular biosensors were developed using various sensing mechanisms.[7,8] Among these, the unimolecular FRET-based PIP_3 reporter Fllip contains a plasma membrane targeting motif, a PIP_3 binding PH domain flanked by a FRET pair, and an engineered diglycine-based hinge installed in the biosensor in such a way that, when the PH domain binds to PIP_3, a conformational change in the probe occurs through the hinge, altering FRET.[7] On the other hand, the FRET-based sensor InPAkt utilized a different sensing mechanism based on competition between a negatively charged pseudo-ligand and endogenous phosphoinositides for binding to the PH domain of Akt, which binds to $PI(3,4)P_2$ and PIP_3, thus defining the specificity of the sensor.[9] This way, the phosphoinositide-binding-induced conformational change does not require specific anchoring of the biosensor and the sensor can be targeted to different compartments.

In this study, inspired by the pseudo-ligand-based design of InPAkt, we developed a PLC-based PIP_2 Reporter (PlcR) by replacing the PH_{Akt} domain in InPAkt with the PH domain of phospholipase Cδ1 that has been shown to exhibit high affinity and specificity for PIP_2 over other phosphoinositides.[10] To further aid the examination of the signaling dynamics of different phosphoinositides and other critical signaling pathways, we engineered intensity-based versions of PIP_2 and 3-phosphoinositide biosensors that can be co-imaged in single living cells. The intensity-based biosensors have a smaller footprint within the usable spectrum, compared to FRET-based sensors, and can be used in combination with multiple other fluorescent biosensors. In comparison to conventional techniques for studying phosphoinositides such as whole-cell-patch-clamp,[11] these newly developed biosensors showed compelling advantages in revealing real-time phosphoinositide signaling dynamics in live cells.

RESULTS AND DISCUSSION

In order to generate a genetically encodable PIP_2 sensor that is also targetable, we first set out to apply the pseudo-ligand design to develop a new FRET-based biosensor for PIP_2. In the new PIP_2 reporter, the sensing unit consists of the PH domain from PLCδ1 ($PH_{PLC\delta1}$), which exhibits high specificity and binding affinity to PIP_2, and a negatively charged pseudo-ligand that can bind to PH domains, the same as in InPAkt. This acidic motif derived from the protein nucleolin has been shown to exhibit relatively high binding affinity for the IRS-1 and IRS-2 PH domains, with an IC_{50} value of <10 nM in a competition experiment.[12] Binding is thought to be facilitated by a positively charged pocket found in these and most structurally related PH domains (see Figure S1 in the Supporting Information), which interacts with the negatively charged head groups of phosphoinositides such as PIP_2 and

PIP_3.[13] These properties led us to utilize this sequence as the pseudo-ligand for InPAkt.[9] While PH_{Akt} binds PIP_3 with nanomolar affinity,[14] the binding affinity of $PH_{PLC\delta1}$ for PIP_2 is orders of magnitude weaker ($K_d \approx 2\ \mu M$).[15] Nevertheless, the different affinities of PH domains for phosphoinositides have evolved based on the relative abundance of these phosphoinositides in the cell membrane; thus, the pseudo-ligand was expected to perform similarly with $PH_{PLC\delta1}$, since the concentrations of PIP_2 in the plasma membrane are also orders of magnitude higher, compared with PIP_3.

Also similar to InPAkt, this biosensor is constructed with its sensing unit sandwiched between a pair of fluorescent proteins as FRET donor and acceptor connected via flexible linkers (see Figures 1A and 1B). In the presence of PIP_2, the phosphoinositide is expected to compete off the pseudo-ligand and induce a conformational change within the biosensor, leading to a change in FRET efficiency that can be monitored by fluorescence microscopy (Figure 1A). As a result, changes in FRET measured as the ratio of yellow emission over cyan emission with cyan excitation can be used to quantify real-time PIP_2 signaling dynamics in live cells. We named this biosensor PlcR: PLC-based PIP_2 Reporter. PlcR was targeted to the plasma membrane, using a lipid modification motif from Lyn kinase (Figure 1B). Stimulation by acetylcholine induced an immediate decrease in yellow/cyan emission ratio in Cos7 cells co-expressing the G_q-coupled muscarinic M_3 acetylcholine receptor (n = 12), but not in the M_3-absent cells (n = 8) (Figure 1C) or in M_3-expressing cells transfected with a $PlcR^{K30/32L}$ mutant that disrupts PIP_2 binding (see Figure S2 in the Supporting Information). Activation of the M_3 receptor leads to G_q-mediated activation of PLC and degradation of PIP_2, and the M3 receptor-dependent responses suggested that PlcR is able to report PIP_2 changes in real time. Activation of PLC causes hydrolysis of PIP_2 into IP_3, which, in turn, triggers Ca^{2+} release from ER to cytosol. When co-imaged with the red fluorescent protein-based Ca^{2+} indicator RCaMP,[16] PlcR showed acetylcholine-stimulated responses in M_3-expressing cells, but not in M_3-absent cells, which were temporally correlated with Ca^{2+} spikes, consistent with the known dynamics of PLC-mediated PIP_2 hydrolysis (see Figures S3 and S4 in the Supporting Information).[11] Overall, these data suggest that the pseudo-ligand-based design is generalizable and can be applied to develop a genetically encoded PIP_2 reporter, PlcR.

Often times, it is beneficial to monitor multiple signaling parameters simultaneously to gain information on how different signaling steps or paths intertwine with each other to regulate cell functions. FRET-based reporters utilize two fluorescent proteins and therefore limit the number of additional fluorescent reporters that can be imaged in the same cells without spectral interference. Intensity-based, single-color biosensors provide several advantages for fluorescence imaging. In terms of the fluorescent readout, they have a smaller footprint within the usable spectrum, compared to FRET sensors, making it possible to monitor more parameters simultaneously. In addition, the hardware requirement is simpler compared to FRET imaging, and the data analysis is straightforward. Therefore, we set out to develop a single-color biosensor for phosphoinositides using the same sensing unit as PlcR. We tested the recently developed dimerization-dependent FPs (ddFPs), replacing the FRET pair in PlcR with ddGFP-A and ddFP-B (see Figures 2A and 2B).[17] These proteins show low fluorescence when spatially separated but when moved into close proximity, ddFP-B dimerizes with ddGFP-A and induces an increase in fluorescence. Given the successful

design of FRET-based PlcR, we hypothesized that the conformational change of the sensing unit, induced by PIP_2 binding-trigged displacement of the pseudo-ligand, can be translated into a change in fluorescence intensity in this case (Figure 2A). When tested in Cos7 cells expressing the muscarinic M_3 receptor, this ddFP-based PIP_2 indicator (dPlcR) showed a decrease in green fluorescence intensity upon acetylcholine stimulation, exhibiting similar kinetics as reported by PlcR, while a $dPlcR^{K30/32L}$ negative-control mutant showed no response (Figure 1C and Figure S5 in the Supporting Information). dPlcR responses were also temporally correlated with Ca^{2+} release from the ER, monitored by RCaMP in the same cells (Figure S6 in the Supporting Information) and were abolished by omission of the M_3 receptor (Figure S7 in the Supporting Information), suggesting the intensity change of dPlcR specifically reflects PIP_2 level changes.

M_3-receptor-mediated PIP_2 hydrolysis produces IP_3 that leads to Ca^{2+} influx and in parallel also produces DAG that turns on Protein Kinase C. To further demonstrate the advantages of such a single-color PIP_2 reporter in multi-parameter imaging, we designed an experiment to monitor PIP_2 levels, Ca^{2+} concentrations, and PKC activity using three reporters, dPlcR, RCaMP and sapphireCKAR,[18] respectively, in the same cells. SapphireCKAR contains circularly permuted T-Sapphire sandwiched between a PKC substrate and a phosphoamino acid-binding domain (PAABD), where PKC-mediated phosphorylation of the substrate causes binding by the PAABD, leading to a decrease in T-Sapphire fluorescence. As shown in Figure 2D and Figure S8 in the Supporting Information, in Cos7 cells expressing the M_3 receptor treated with acetylcholine, PIP_2 depletion at the plasma membrane was coupled to instant increases in Ca^{2+} and PKC activity, suggesting that both IP_3 and DAG production were initiated immediately after PLC activation on the plasma membrane. As expected, no responses were observed in Cos7 cells lacking M_3 receptors (Figure S9 in the Supporting Information). In summary, by extending the design of PlcR, we engineered an intensity-based green PIP_2 sensor, dPlcR, utilizing dimerization-dependent green fluorescent protein as its reporting unit and demonstrated that dPlcR can report membrane PIP_2 changes triggered by both overexpressed and endogenous Gq-coupled receptors (Figure 2 and Figure S10 in the Supporting Information) via changes in green fluorescence intensity. Such a single-color dPlcR can be easily employed to co-image with other reporters to monitor and dissect multiple signaling parameters in single cells.

Activation of G_q-coupled receptors is known to induce a large decrease in PIP_2 via PLC. On the other hand, PIP_2 is also the substrate for generating PIP_3, an important lipid second messenger. For example, activation of various growth factor receptors, including EGF receptor (EGFR), is known to activate PI3K to convert PIP_2 to PIP_3. However, PIP_2 levels must be properly maintained at the plasma membrane, as this lipid itself plays an important role in channel function and membrane dynamics.[1] To probe the inter-relationships between PIP_2 and PIP_3, we set out to develop a 3-phosphoinositide indicator that can be co-imaged with dPlcR. Based on our experience with the development of dPlcR, we reasoned that the use of ddFPs as the reporting unit could be coupled with the sensing unit consisting of PH_{Akt} and pseudo-ligand from the previously developed 3-phosphoinosi-tide reporter InPAkt to give rise to an intensity-based single-color 3-phosphoinositide indicator. We constructed this biosensor by replacing the FRET pair in InPAkt with ddRFP-A and ddFP-B, the red version of dimerization-dependent FPs. We named this biosensor dInPAkt (see Figures 3A and 3B).

When Cos7 cells expressing dInPAkt were treated with EGF, we observed a decrease in red fluorescence intensity (see Figure 3C and Figure S11 in the Supporting Information), with similar kinetics to those observed using InPAkt (Figure S12 in the Supporting Information). This EGF-induced response was absent in cells expressing a dInPAkt$^{R23/25A}$ negative control (Figure S13 in the Supporting Information) and was also abolished by pretreating cells with the PI3K inhibitors LY294002 and Wortmannin prior to imaging (Figure 3C and Figure S14 in the Supporting Information), a condition shown to block EGF-induced InPAkt responses as well (see Figure S12).[19,20] These results suggest that changes in dInPAkt intensity reflect PI3K-dependent changes in plasma membrane 3-phosphoinositide levels, where a decrease in dInPAkt RFP fluorescence intensity indicates an increase in 3-phosphoinositides.

It has been suggested that PI3K utilizes a pre-existing PIP_2 pool for PIP_3 synthesis, as the cellular concentration of PIP_2 is at least 2 orders of magnitude higher than that of PIP_3.[21,22] This would imply that PIP_2 levels will not change significantly upon growth factor-stimulated PI3K activation. However, recent findings suggest that a substantial fraction of pre-existing PIP_2 is sequestered and unavailable for use by PI3K, thus requiring *de novo* PIP_2 generation to be coordinated with PI3K activation and PIP_3 generation at a specific cellular compartment.[23] In any case, it is unclear how PI3K activation impacts membrane PIP_2 levels and how PIP_2 and PIP_3 levels are inter-related within local membrane compartments. Our newly developed green PIP_2 reporter dPlcR and red 3-phosphoinositide reporter dInPAkt now provide a means for simultaneously monitoring PIP_2 and PIP_3 at any desired membrane compartments. As shown in Figure 3D, when both reporters are targeted to the plasma membrane, EGF stimulation triggered a decrease in dInPAkt intensity, representing an increase in cellular 3-phosphoinositide levels, along with a reciprocal response from dPlcR with very similar kinetics, indicating that PIP_3 formation does decrease local PIP_2 levels. Interestingly we observed considerable cell-to-cell variability in the re-establishment of equilibrated PIP_2 levels, as indicated by the reversal of fluorescence changes (Figure S11). Meanwhile, pretreating cells with PI3K inhibitors resulted in significantly dampened/attenuated PIP_2 decreases and 3-phosphoinositide increases (see Figure 3E, as well as Figures S11 and S14). In summary, our results show that the dPlcR-dInPAkt co-imaging system can successfully report PI3K-dependent 3-phosphoinositide formation and PIP_2 depletion simultaneously on the plasma membrane and at other potential subcellular compartments, further demonstrating the advantages of multiplexed imaging and single-color reporters.

In this study, we successfully developed a series of phosphoinositide reporters that exhibit the following advantages in examining lipid signaling in living systems: (1) genetically encodable with low toxicity and high preservation of the native cellular environment, (2) spatially targetable to enable cellular subcellular location-specific signaling analysis, and (3) multiple color and readout options to suit different microscope apparatus/settings and multiplexed imaging. Importantly, we have demonstrated that the design principles of this series of reporters are highly generalizable and can be applied for the development and optimization of new sensors. By replacing the FRET-based reporting unit of InPAkt with a dimerization-dependent FP pair, we engineered a single-color version of InPAkt–dInPAkt. By utilizing the reporting unit and changing the sensing unit to a PIP_2 binding domain, we

also developed a new family of PIP_2 reporters. Multiplexed imaging revealed PIP_3 production is highly correlated with PIP_2 deletion in the same membrane compartment, consistent with the idea that a substantial fraction of pre-existing PIP_2 is unavailable for use by PI3K. Overall, development of these reporters has not only expanded the toolbox for studying phosphoinositide signaling in its native cellular environment but also showcased the modular design of these genetically encoded fluorescent biosensors that makes them generalizable and adaptable to a variety of different targets and applications.

EXPERIMENTAL PROCEDURES

Construct Generation.

Standard cloning procedures were performed, including PCR with specific primers using Phusion polymerase (Catalog No. F530S, Thermo Fisher Scientific), restriction endonuclease digestion, and ligation using T4 DNA ligase (Catalog No. 15224017, Thermo Fisher Scientific). DH5α *E. coli* cells were employed for cloning and amplification of plasmids. The PH domains of Akt and PLCδ1 were cloned from mRNA from *Rattus norvegicus* brain tissue. First, mRNA was isolated using the RNeasy Kit (Catalog No. 74106, Qiagen), then the OneStep RT-PCR Kit (Catalog No. 220213, Qiagen) was used with specific primers to generate the DNA fragments, which were subsequently cloned into the plasmid pCR2.1 using the TOPO TA cloning kit (Catalog No. K457501, Thermo Fisher Scientific). For subsequent constructs, the pcDNA3 vector was utilized. In order to assemble Lyn-targeted PlcR, eYFP, $PH_{PLC\delta1}$, and eCFP were inserted into pcDNA3 using the restriction enzymes *Kpn*I, *Bam*HI, *Eco*RI, and NotI. The sequence for the Lyn-tag (atgggc gcatcaagagcaagcgcaaggacaag) and the sequence for the pseudo-ligand (ggcggtagcgtggcagaagaggaagatgacgaggaagaggacgaggacgatggcggcagc) were added N-terminally to eYFP and eCFP, respectively, utilizing extended primers for the PCR. For the construction of Lyn-targeted dPlcR and dInPAkt, a pcDNA3 vector with a modified multiple cloning site and a Lyn-tag upstream of a *Bam*HI restriction site was employed. The fragments of ddGFP-A or ddRFP-A, $PH_{PLC\delta1}$ or PH_{Akt}, the pseudo-ligand, and ddFP-B were subcloned using the restriction enzymes *Bam*HI, SphI, *Sal*I, SacI, and XbaI. An expression plasmid for the rat M_3 receptor was available from a previous project.[11] $PlcR^{K30/32L}$, $dPlcR^{K30/32L}$, and $dInPAkt^{R23/25A}$ negative control mutant sensors were generated via PCR mutagenesis and Gibson assembly. All constructs were verified by sequencing. Restriction enzymes were purchased from New England BioLabs.

Cell Culture and Transfection.

Cos7 cells were grown in Dulbecco modified Eagle medium (DMEM, Catalog No. 11965084, Fisher Scientific) containing 5 g/L glucose and supplemented with 10% (v/v) fetal bovine serum (FBS, Catalog No. 35011CV, Fisher Scientific) and 1% (v/v) penicillin/streptomycin (Pen-Strep) Catalog No. 15140122, Thermo Scientific), maintained at 37 °C in an atmosphere of 5% CO_2. HeLa cells were grown in DMEM (Fisher Scientific) containing 1 g/L glucose and supplemented with 10% (v/v) FBS (Fisher Scientific) and 1% (v/v) Pen-Strep (Thermo Scientific), maintained at 37 °C in an atmosphere of 5% CO_2. Cells were seeded in sterile 35 mm glass-bottom imaging dishes and transfected at a confluency of ~70%, using PolyJet In Vitro DNA Transfection Reagent (Catalog No. SL100688,

Signagen), following the manufacturer's protocol. After incubation for 6 h, growth media was removed and changed to fresh complete growth media. After 48 h of transfection, cells were washed twice with Hank's Balanced Salt Solution (Gibco HBSS, Catalog No. 14025092, Thermo Scientific) buffer and subsequently imaged in HBSS buffer at room temperature (RT). Cells used in experiments with EGF stimulation were serum-starved overnight prior to imaging. Acetylcholine (Catalog No. A2661, Sigma), histamine (Catalog No. H7250, Sigma), hEGF (Catalog No. E9644, Sigma), PI3K inhibitor LY294002 (Catalog No. L7962, LA Laboratories) and wortmannin (Catalog No. W-2990, LC Laboratories) were added as indicated.

Epifluorescence Microscopy and Image Analysis.

Images were acquired in darkness on a Zeiss AxioObserver Z7 microscope (Carl Zeiss) that was equipped with a 40×/1.4 NA objective and a Prime95B sCMOS camera (Photometrics) controlled by MetaFluor7.7 software (Molecular Devices). GFP intensity for dPlcR was imaged using a Model 480DF20 excitation filter (Omega Optics), a Model 505DRLP dichroic mirror (Omega Optical), and a Model 535DF50 emission filter (Chroma Technologies). RFP intensity for RCaMP and dInPAkt was imaged using a Model 572DF35 excitation filter, a Model 594DRLP dichroic mirror, and a Model 645DF75 emission filter. T-Sapphire intensity for sapphireCKAR was imaged using a Model 405DF20 excitation filter, a Model 455DRLP dichroic mirror, and a Model 535DF50 emission filter (Chroma Technologies). Dual cyan/yellow emission ratio imaging for InPAkt was performed using a 420DF20 excitation filter/455DRLP dichroic mirror/473DF24 emission filter for CFP intensity, 420DF20 excitation filter/455DRLP dichroic mirror/535DF25 emission filter for the FRET intensity, and 495DF10 excitation filter/515DRLP dichroic mirror/535DF25 emission filter for YFP intensity. All filter sets were managed by an LEP Model MAC600 control module (Ludl Electronic Products, Ltd.). Exposure times ranged between 50 ms and 500 ms. Images were acquired every 20–30 s, and stimulus in each experiment was added as indicated with no pause during image acquisition. InPAkt FRET ratios were quantified as FRET intensity over CFP intensity.

Imaging data was analyzed and processed using MetaFluor software. Time courses were normalized by dividing the background (cell free region)-subtracted fluorescence intensity or FRET ratio at any given time t by the basal value at t_0 (the time point immediately prior to stimulus addition), e.g., R/R_0 for FRET responses or $\Delta F/F_0 = (F - F_0)/F_0$ for intensity responses. Importantly, because the fluorescence intensities of dInPAkt and sapphireCKAR change inversely with cellular levels of 3-phosphoinositides and PKC activity, respectively, dInPAkt and sapphireCKAR responses are correspondingly plotted as $-\Delta F/F_0$.

Supplementary Material

Refer to Web version on PubMed Central for supplementary material.

ACKNOWLEDGMENTS

This work was supported by NIH R35 CA197622 and R01 GM111665 (to J.Z.).

REFERENCES

(1). Balla T (2013) Phosphoinositides: Tiny Lipids with Giant Impact on Cell Regulation. Physiol. Rev 93, 1019–1137. [PubMed: 23899561]

(2). Falkenburger BH, Jensen JB, and Hille B (2010) Kinetics of PIP2Metabolism and KCNQ2/3 Channel Regulation Studied with a Voltage-Sensitive Phosphatase in Living Cells. J. Gen. Physiol 135, 99–114. [PubMed: 20100891]

(3). Chalhoub N, and Baker SJ (2009) PTEN and the PI3-Kinase Pathway in Cancer. Annu. Rev. Pathol.: Mech. Dis 4, 127–150.

(4). Greenwald EC, Mehta S, and Zhang J (2018) Genetically Encoded Fluorescent Biosensors Illuminate the Spatiotemporal Regulation of Signaling Networks. Chem. Rev 118, 11707–11794. [PubMed: 30550275]

(5). Halet G (2005) Imaging Phosphoinositide Dynamics Using GFP-Tagged Protein Domains. Biol. Cell 97, 501–518. [PubMed: 15966865]

(6). van der Wal J, Habets R, Várnai P, Balla T, and Jalink K (2001) Monitoring Agonist-Induced Phospholipase C Activation in Live Cells by Fluorescence Resonance Energy Transfer. J. Biol. Chem 276, 15337–15344. [PubMed: 11152673]

(7). Sato M, Ueda Y, Takagi T, and Umezawa Y (2003) Production of PtdInsP3 at Endomembranes Is Triggered by Receptor Endocytosis. Nat. Cell Biol 5, 1016–1022. [PubMed: 14528311]

(8). Nishioka T, Aoki K, Hikake K, Yoshizaki H, Kiyokawa E, and Matsuda M (2008) Rapid Turnover Rate of Phosphoinositides at the Front of Migrating MDCK Cells. Mol. Biol. Cell 19, 4213–4223. [PubMed: 18685081]

(9). Ananthanarayanan B, Ni Q, and Zhang J (2005) Signal Propagation from Membrane Messengers to Nuclear Effectors Revealed by Reporters of Phosphoinositide Dynamics and Akt Activity. Proc. Natl. Acad. Sci. U. S. A 102, 15081–15086. [PubMed: 16214892]

(10). Lemmon MA (2007) Pleckstrin Homology (PH) Domains and Phosphoinositides. Biochem. Soc. Symp 74 (74), 81–93.

(11). Hertel F, Switalski A, Mintert-Jancke E, Karavassilidou K, Bender K, Pott L, and Kienitz M-C (2011) A Genetically Encoded Tool Kit for Manipulating and Monitoring Membrane Phosphatidylinositol 4,5-Bisphosphate in Intact Cells. PLoS One 6, No. e20855.

(12). Burks DJ, Wang J, Towery H, Ishibashi O, Lowe D, Riedel H, and White MF (1998) IRS Pleckstrin Homology Domains Bind to Acidic Motifs in Proteins. J. Biol. Chem 273, 31061–31067. [PubMed: 9813005]

(13). Razzini G, Ingrosso A, Brancaccio A, Sciacchitano S, Esposito DL, and Falasca M (2000) Different Subcellular Localization and Phosphoinositides Binding of Insulin Receptor Substrate Protein Pleckstrin Homology Domains. Mol. Endocrinol 14, 823–836. [PubMed: 10847585]

(14). Rowland MM, Gong D, Bostic HE, Lucas N, Cho W, and Best MD (2012) Microarray Analysis of Akt PH Domain Binding Employing Synthetic Biotinylated Analogs of All Seven Phosphoinositide Headgroup Isomers. Chem. Phys. Lipids 165, 207–215. [PubMed: 22178158]

(15). Hirose K, Kadowaki S, Tanabe M, Takeshima H, and Iino M (1999) Spatiotemporal Dynamics of Inositol 1,4,5-Trisphosphate That Underlies Complex Ca^{2+} Mobilization Patterns. Science 284, 1527–1530. [PubMed: 10348740]

(16). Akerboom J, Carreras Calderón N, Tian L, Wabnig S, Prigge M, Tolö J, Gordus A, Orger MB, Severi KE, Macklin JJ, Patel R, Pulver SR, Wardill TJ, Fischer E, Schüler C, Chen TW, Sarkisyan KS, Marvin JS, Bargmann CI, Kim DS, Kügler S, Lagnado L, Hegemann P, Gottschalk A, Schreiter ES, and Looger LL (2013) Genetically Encoded Calcium Indicators for Multi-Color Neural Activity Imaging and Combination with Optogenetics. Front. Mol. Neurosci 6, 2. [PubMed: 23459413]

(17). Alford SC, Ding Y, Simmen T, and Campbell RE (2012) Dimerization-Dependent Green and Yellow Fluorescent Proteins. ACS Synth. Biol 1, 569–575. [PubMed: 23656278]

(18). Mehta S, Zhang Y, Roth RH, Zhang J-F, Mo A, Tenner B, Huganir RL, and Zhang J (2018) Single-Fluorophore Biosensors for Sensitive and Multiplexed Detection of Signalling Activities. Nat. Cell Biol 20, 1215–1225. [PubMed: 30250062]

(19). Vlahos CJ, Matter WF, Hui KY, and Brown RF (1994) A Specific Inhibitor of Phosphatidylinositol 3-Kinase, 2-(4-Morpholinyl)-8-Phenyl-4H-1-Benzopyran-4-One (LY294002). J. Biol. Chem 269, 5241–5248. [PubMed: 8106507]

(20). Arcaro A, and Wymann MP (1993) Wortmannin Is a Potent Phosphatidylinositol 3-Kinase Inhibitor: The Role of Phosphatidylinositol 3,4,5-Trisphosphate in Neutrophil Responses. Biochem. J 296, 297–301. [PubMed: 8257416]

(21). Insall RH, and Weiner OD (2001) PIP3, PIP2, and Cell Movement–Similar Messages, Different Meanings? Dev. Cell 1, 743–747. [PubMed: 11740936]

(22). Stephens LR, Jackson TR, and Hawkins PT (1993) Agonist-Stimulated Synthesis of Phosphatidylinositol(3,4,5)-Trisphosphate: A New Intracellular Signalling System? Biochim. Biophys. Acta, Mol. Cell Res 1179, 27–75.

(23). Choi S, Houdek X, and Anderson RA (2018) Phosphoinositide 3-Kinase Pathways and Autophagy Require Phosphatidylinositol Phosphate Kinases. Adv. Biol. Regul 68, 31–38. [PubMed: 29472147]

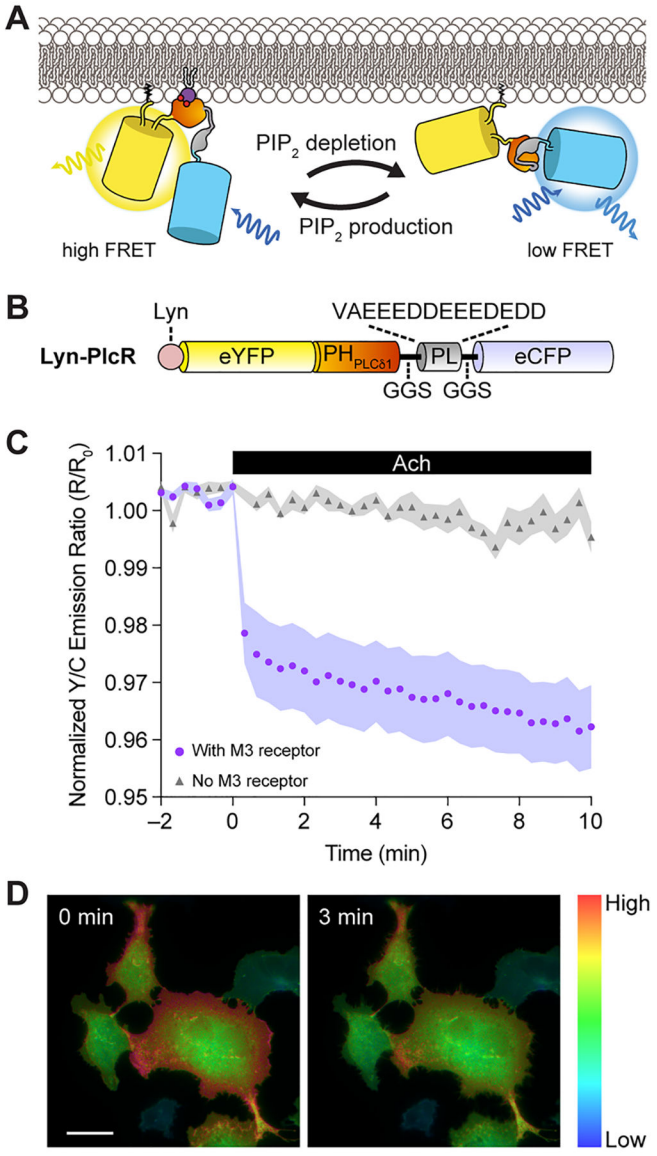

Figure 1.

Development and characterization of FRET-based PIP_2reporter PlcR. (A) Schematic representation of phospholipase Cδ1 (PLCδ1)-based PIP_2 reporter, PlcR. A negatively charged pseudo-ligand (PL) and PIP_2 compete for binding to the PH domain of PLCδ1 ($PH_{PLC\delta1}$), resulting in a conformation change upon PIP_2 depletion, where the reporter adopts a low FRET efficiency conformation between the two fluorescent proteins, enhanced Yellow Fluorescent Protein (eYFP) and enhanced Cyan Fluorescent Protein (eCFP). (B) Graphic illustration of the domain structure of plasma membrane-targeted Lyn-PlcR. (C) Time course of the normalized yellow-over-cyan (Y/C) emission ratio in Cos7 cells expressing Lyn-PlcR with (circles, $n = 12$) or without (triangles, $n = 8$) co-expression of the G_q-coupled M_3 receptor upon acetylcholine (Ach, 10 μM) stimulation at $t = 0$ min. Images were acquired every 20 s. Shaded areas represent SEM. Single cell traces co-monitored with the Ca^{2+} indicator RCaMP are shown in Figures S3 and S4. (D) Pseudo-color images

showing the FRET ratio changes in Cos7 cells expressing Lyn-PlcR before and after acetylcholine stimulation, where warmer colors indicate high plasma membrane PIP_2 levels and cooler colors indicate low PIP_2. Scale bar = 10 μm.

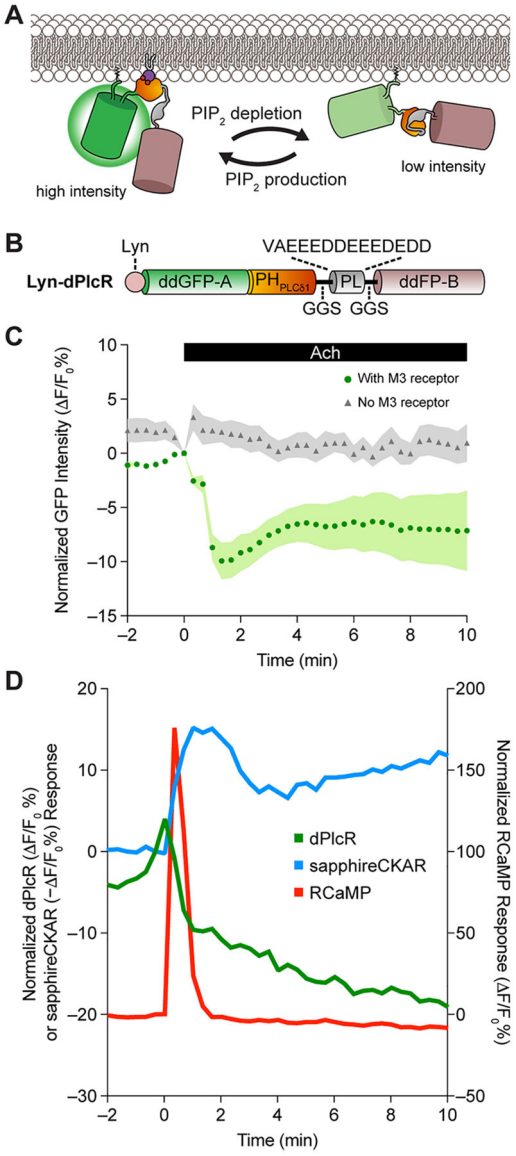

Figure 2.

Development and characterization of fluorescence intensity-based PIP_2 reporter dPlcR. (A) Schematic representation of dPlcR, where $PH_{PLC\delta1}$ binding to membrane PIP_2 leads to a decrease in the distance between the two dimerization-dependent GFP monomers ddGFP-A (green, dim) and ddFP-B (dark) and an increase in fluorescence intensity, as a result of ddFP heterodimerization (green, bright). Depletion of membrane PIP_2 will thus lead to decreased green fluorescence intensity. (B) Graphic illustration of the domain structure of plasma membrane-targeted Lyn-dPlcR. (C) Time course of normalized Lyn-dPlcR green fluorescence intensity in Cos7 cells with (circles, $n = 8$) or without (triangles, $n = 8$) G_q-coupled M_3 receptor co-expression upon acetylcholine (10 μM) stimulation at $t = 0$ min. Images were acquired every 20 s. Shaded areas represent SEM. Single-cell traces co-monitored with the Ca^{2+} indicator RCaMP are shown in Figures S6 and S7 in the Supporting Information. (D) Time course of PIP_2 depletion (monitored by Lyn-dPlcR in green),

intracellular Ca^{2+} influx (RCaMP in red), and PKC activity (sapphireCKAR in blue) in M_3 receptor-expressing Cos7 cells upon acetylcholine (Ach, 10 μM) addition at $t = 0$ min. Plots show representative traces from a single cell. Additional single-cell traces from independent experiments are shown in Figure S8 in the Supporting Information ($n = 5$), and responses from cells without M_3 receptor are shown in Figure S9 in the Supporting Information ($n = 9$) as a negative control.

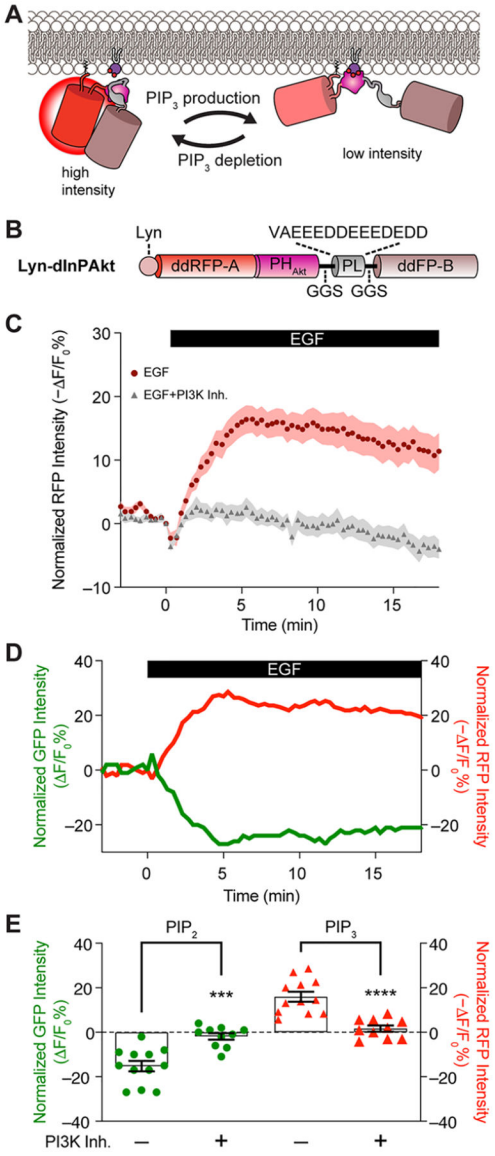

Figure 3.

Development of fluorescence intensity-based reporter dInPAkt and multiplexed imaging of phosphoinositide dynamics. (A) Schematic representation of dInPAkt, where PH_{Akt} binding to membrane 3-phosphoinositides leads to an increase in distance between the two dimerization-dependent RFP monomers ddRFP-A (red, bright) and ddFP-B (dark) and a decrease in fluorescence intensity, because of the loss of ddFP heterodimerization (red, dim). Therefore, the production of 3-phosphoinositide membranes will thus lead to a decrease in red fluorescence intensity. (B) Graphic illustration of the domain structure of the Lyn-targeted dInPAkt.(C) Time course of normalized dInPAkt red fluorescence intensity in response to EGF stimulation (100 ng/mL) in Cos7 cells with (triangles, $n = 9$) or without (circles, $n = 11$) PI3K inhibitor preincubation. Images were acquired every 20 s. Shaded areas represent SEM (D) Time course of PIP_2 depletion (monitored by Lyn-dPlcR, shown in green) and production of 3-phosphoinositides (Lyn-dInPAkt, shown in red) in Cos7 cells in

response to EGF. Plots shown are representative single-cell traces. Additional single-cell traces from independent experiments are shown in Figures S11 (no pretreatment) and S14 (with PI3K preinhibition) in the Supporting Information. (E) Statistical analysis of membrane PIP_2 (circles) and 3-phosphoinositide (diamonds) levels after 5 min of EGF stimulation (100 ng/mL) in Cos7 cells with (+) or without (−) PI3K preinhibition, quantified from single-cell traces in Figures S11 and S14. [Legend: (***) $p < 0.001$ and (****) $p < 0.0001$, from Student's *t*-test.]